Article

Ion migration mechanisms in the early stages of drying and degradation of oil paint films

Check for updates

Margherita Gnemmi[1], Laura Fuster-Lòpez[2], Marion Mecklenburg[3], Alison Murray[4], Sarah Sands[5], Greg Watson[5] & Francesca Caterina Izzo [1] ✉

The study of film-formation processes of oil paints has been extensively addressed over the last decade and the influence of metal ions in the drying and degradation stages of oil paints has been demonstrated. This research aimed to determine a suitable methodology for monitoring the early drying stages of selected commercial oil paint films and to gain an insight into the migration mechanisms of material degradation taking place between adjacent paint films, with special attention to the influence of the lead white. For this purpose, a hybrid approach was adopted to characterize the composition of the paint and highlight failure mechanisms in the paint films through a wide range of time. The methods included scribe tests, percentage weight variation (ΔW%), attenuated reflectance Fourier transform infrared spectrophotometry (ATR-FTIR), gas chromatography-mass spectrometry (GC-MS), and thermal analysis with differential scanning calorimetry (TG-DSC). The results show how metal ions interact with the oil binder and the pigment in the adjacent paint film: the transverse migration of lead white is shown to affect the reactivity of polyunsaturated triglycerides, increasing the rate of oxygen uptake and promoting the formation of radicals and bonds between polymer chains, depending on the pigment with which it interacts.

Artists' oil paints are complex systems[1–4]. Their composite structure made of materials with different chemical and mechanical properties, and the interactions taking place between these layers at the interface are sources of stress within the structure, often leading to different degradation phenomena such as cracks, delamination, and protrusions[5,6].

In the last decade, research has provided a deep understanding of the chemistry of oils, their drying, and degradation[7–11]. Specifically, metal soap formation and its effects on the paint structure have been investigated in depth as evidenced by the considerable amount of specific literature available[6,12–15].

A detailed study of the variety and extent of damage typically found on oil-painted surfaces reveals the complexity of the degradation phenomena involved, mostly as a result of synergistic circumstances and where the intrinsic nature of the paint materials plays a major role[16–18].

Recent research has shown that material degradation found in oil paintings can be selective as a function of specific pigments and therefore limited to specific colour areas. This is usually the case of areas where metal-based pigments (e.g. lead, zinc, or cobalt-based pigments) have been used

and where the damage observed is often due to the combined effect of the chemistry of the pigments and their interaction with the oil binding medium[6,12,13,19–24].

In 2010, Mecklenburg et al. performed X-ray microanalysis on a cross-section of mock-up systems containing two paint layers and demonstrated that metal ions are not only capable of migrating throughout a given paint layer but are also sufficiently mobile to migrate from one paint layer to an adjacent one in a painting, improving or degrading it[10,17]. Certain underlying grounds or specific combinations of paint layers seem to be able to improve the cohesive properties of a paint layer, thus making it less vulnerable to degradation[10,17]. In addition, an oil paint layer can influence the other adjacent layers in both positive and negative ways: some metal ions are able to influence drying rates and fatty acid anions, affecting stiffness or flexibility and forming accretions; while others are not able to contribute to the formation of a durable film, causing detrimental effects such as brittleness and even delamination of the paint layers.

These changes in properties may have many practical implications for both conservators (e.g. understanding the sensitivity of painted surfaces to

[1]Ca' Foscari University of Venice, Department of Environmental Sciences, Informatics and Statistics, Venice, Italy. [2]Universitat Politècnica de València, Instituto Universitario de Restauración del Patrimonio, Valencia, Spain. [3]Smithsonian Museum Conservation Institute, Suitland, USA. [4]Queen's University, Art Conservation Program, Department of Art History and Art Conservation, Kingston, Canada. [5]Golden Artists Paints, New Berlin, USA. ✉e-mail: fra.izzo@unive.it

Article

Table 1 | Information about the selected pigment: product name; colour index Generic name (CI) to describe a commercial product according to its recognized use class; opacity to define the physical property that indicates the quality of light transmission by the surface of a material; grind to indicate the size of the pigment mass

MANUFACTURER	PRODUCT NAME	CI NAME	DESCRIPTION	OPACITY	GRIND
GOLDEN ARTIST COLORS	Cobalt Blue	PB28	Oxides of Cobalt and Aluminium	Semi-opaque	Very Fine
	Raw Umber	PBr7	Natural Iron Oxide containing Manganese	Semi-opaque	Fine
	Burnt Umber	PBr7	Calcined Natural Iron Oxide containing Manganese	Semi-opaque	Fine
	Burnt Sienna	PR102	Calcined Natural Hydrated Iron Oxide	Semi-opaque	Fine
	Raw Sienna	PY43	Natural Hydrated Iron Oxide	Semi-opaque	Fine
	Red Iron Oxide	PR101	Iron Oxide	Semi-opaque	Very Fine
	Yellow Ochre	PY43	Natural Hydrated Iron Oxide	Semi-opaque	Fine
	Zinc White	PW4	Zinc Oxide	Semi-opaque	Very fine
	Lead White	PW1	Basic Lead Carbonate	Opaque	Very fine
	Titanium White	PW6	Titanium Dioxide Rutile	Opaque	Very fine

cleaning treatments) and paint manufacturers (e.g. improving the long-term properties of paints). However, it has also been observed that ion migration can cause paints to become brittle or change the visual appearance of oil films over time, e.g. the appearance and properties of the resulting oil colours[20,25,26]. Ion migration could therefore explain several degradation phenomena observed in oil paintings, which have yet been understood or studied and for which several experiments are currently being carried out at the SOLEIL sychrotron by Kéckicheff et al. [27].

A study of four contemporary paintings by Picasso discussed these interactions thorough a detailed characterization of the painting materials and the cracks present on the painted surface. The morphology of the crack network varied according to the stratigraphy of the painted structure, i.e. how the artist had built up the paint layers and how these had interacted with each other[28]. This particular case study highlighted how pigment composition can govern the degradation phenomena of oil paint films, as the ongoing degradation phenomena were closely linked to the chemical interaction between pigment and binding medium. This suggests that the migration of metal ions may not only lead to the formation of lead soap protrusions and efflorescence in the painted surfaces but may also play a key role in the formation and propagation of cracks within the painted structure.

This research found that the paint film had influenced the development of local cracks observed in the paintings and was attributed to different chemical and physical properties of the paint including the pigments. The fewer cracks found in flesh tones and grey areas were most likely due to active metal ions from lead white forming a more durable paint film. The predominance of lead white resulted in a more open crack network, whereas a massive network of small cracks was observed in the areas without any lead[19–21]. This suggests that the migration of metal ions not only may lead to the formation of lead soaps protrusions and efflorescence in the painted surfaces but may play a key role in the formation and propagation of cracks within the painted structure[28–31]. Some studies have already pointed in this direction[12]. However, the observation in the Picasso's paintings suggests that this migration, usually understood as a vertical migration through layers (i.e. from bottom to top, and then protruding into the surface), may also occur transversely, affecting adjacent coloured areas[17].

To investigate this, several experimental studies were carried out. In 2019, selected oil paints without additives were produced ad hoc for research purposes by Golden Artist Colours (USA) and different sets of samples were cast. (Samples were cast at the Polytechnic University of Valencia, Ca' Foscari University of Venice and at Queen's University in Kingston, Canada. Each team prepared complementary sets of samples in order to be able to correlate the results and to broaden the matrix of pigments studied. This paper only reports the results of the European team. The results of the studies carried out at Queens are forthcoming). Three studies were carried out providing different but complementary perspectives on the same

question. Materials specialists at Golden were conducting some experiments to observe the drying process of some oil paints in order to improve their products: they wanted to understand how the drying process of oil paints could be affected depending on the paint films with which they were in contact. Mecklenburg had shown that two oil paint films can interact and either improve or weaken each other[10,20,24]. Fuster et al. had investigated several case studies where different crack patterns were identified in selective colour areas as a function of the presence of lead compounds[24,28,32]. There were therefore three complementary perspectives looking at the same issues: (a) how pigment–medium interactions occur in oil paints; (b) which are the pigments that induce a more significant influence in adjacent paint layers; and (c) if they do, how do they affect the drying and subsequent stability of oil paint films.

The research presented here was carried out in the framework of the MIMO project (*MIMO-Metal Ion Migration mechanisms in Oil paints drying and degradation*_PID 2019-106616GB-100) which aims to correlate the chemistry of oil paints with mechanical behaviour and degradation phenomena. The main objective was twofold: firstly, to define a multi-analytical methodology capable of observing the interactions between oil and pigment at different drying times, allowing the correlation of the chemistry of oil paints with their drying and film-forming mechanisms. Secondly, to monitor the early stages of drying, curing, and film-formation of selected custom-made oil paint films, both alone and in contact with a lead paint film, in order to understand the extent to which lead ions migrate and influence these processes.

Materials and methods
Preparation of samples
Two sets of samples were prepared using oil paints manufactured by Golden Artist Colours Inc., USA. These paints were produced ad hoc for this research. The selection was a representative range of traditional and common colours commonly used by artists (Table 1) and had Alkali Refined Linseed Oil (ARLO) as the binding medium[33].

The paints are referred to as 'control oils' as they only contain pigment and lipid binders without the addition of additives.

Two different mock-up sets were cast, as described in Table 2: SET1 consisted of a single layer of paint; and SET2 consisted of two layers of oil paint (a coloured oil paint film applied next to a lead white oil paint film). Both sets of samples were cast in 2021.

A BYK-Gardner four-sided applicator with a versatile bar that has multiple gap clearances (50, 100, 150, 200 μm) was used. The samples were cast on Polymex Clear® polyester film (Fig. 1). The polyester film was cut to the required size and placed on a smooth surface with an anchoring system to hold it in place. The paint and the applicator were then placed on the 200 μm side, at the top of the substrate. The applicator was then pushed at

Table 2 | Sets of mock-ups

SETS	TYPE OF SAMPLE			SAMPLES STUDIED	
SET 1	Single	**SINGLE-LAYER** PAINT FILM CAST IN 2021		– Cobalt blue	
				– Raw umber	
				– Burnt umber	
				– Burnt Sienna	
				– Raw Sienna	
				– Red iron oxide	
				– Yellow ochre	
				– Zinc white	
				– Lead white	
				– Titanium white	
SET 2	Side-by-side	**COLOUR** PAINT FILM NEXT TO **LEAD WHITE PAINT FILM** CAST IN 2021		– Cobalt blue	+ Lead white
				– Raw umber	+ Lead white
				– Burnt umber	+ Lead white
				– Burnt Sienna	+ Lead white
				– Raw Sienna	+ Lead white
				– Red iron oxide	+ Lead white
				– Yellow ochre	+ Lead white
				– Zinc white	+ Lead white
				– Titanium white	+ Lead white

Fig. 1 | Application methodology and samples prepared. Graphical representation of the four-sided applicator with versatile bar and different distances (50, 100, 150, 200 μm) used to cast the mockups.
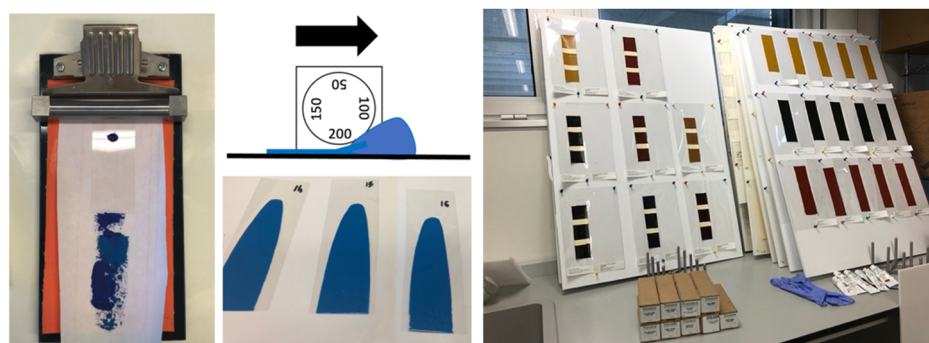
constant pressure and speed (approximately 25 mm/s). The operator selected a gap of 200 μm because, according to the particle size of the pigments in the oil paint tube, this was the optimal gap to obtain homogeneous layers. The samples were stored in the laboratory under stable environmental conditions monitored by a data logger (temperature of 22 °C and relative humidity of 55%).

Experimental methodology

The Scribe Test is a standard test method for evaluating drying or curing during film formation of organic coatings using mechanical recorders (ASTM D5895-20) modified by Golden Artist Colour Inc[34,35]. The test is based on direct observation and was therefore used in a preliminary evaluation phase. The test consists of sliding a wooden stick along a fresh coat of paint. The test is repeated daily until the sliding of the stick no longer leaves any marks ovn the paint film. The operator must maintain the same pressure when sliding the stick so that the observations can be correlated.

In this study, the test was carried out on SET1 and SET2, by the same researcher. The aim was to compare the drying times and processes of different paint films depending on the pigment in their composition and the ageing stage. The comparison of the results made it possible to identify several relevant effects of the influence of lead white when it is applied alongside oil paint films containing other pigments[29,36].

To the best of our knowledge, this is the first scientific study combining the results of the scribe tests with those obtained by the following analytical techniques.

Percentage weight variation is a calculation tool to know the percentage of difference, positive or negative, between two weight measurements, called ΔW%. The purpose of this analysis was to determine the percentage change in weight of the single and side-by-side paint films from the very first moment of the application (0 h) to the time reached their dry-to-the-touch point.

The calculation formula for evaluating the percentage change in weight is given below (1):

$$\Delta W\% = [(W_{f} - W_{i})/W_{i}] \times 100\% \tag{1}$$

Where W_i is the initial value of the weight and W_f is the final weight. In this study, the above mathematical calculation was used to determine the percentage weight variation of the coloured paint layer over time, both from SET1 and SET2. Three replicas were made for each colour of the sets to ensure repeatability.

The paint films were weighed using a technical balance and the measurement was repeated three times to determine the mathematical average. Measurements were taken at the time of application and every 2 h on the first day, every 4 h on the second day, every 8 h on the third day, then daily for the first 2 weeks, and then weekly until the weight stabilized. Once the values of ΔWeight% were obtained, Cartesian graphs were created by placing the time at which the analyses were repeated on the x-axis and the average percentage value on the y-axis.

The purpose of this analysis was to determine the change in the percentage weight of the single and side-by-side paint films from the very first moment of the application (0 h) to the time when they reached their dry-to-the-touch point.

No special preparation was required for the ATR analyses, which were carried out by placing the paint films in direct contact with the crystal. A Bruker Optics Alpha spectrophotometer in ATR mode was used, with a diamond crystal capable of scanning a sample area of 0.75 mm at a depth of approximately 1 micrometre. The spectrometer was equipped with a Pt/SiC globe source, a RockSolid interferometer (with gold mirrors), and a deuterated triglycine sulphate (DLaTGS) detector, operating at room temperature and giving a linear response in the spectral range between 7500 and $375\ cm^{-1}$. Five measuring spots for each sample were acquired in the spectral range between 4000 and $400\ cm^{-1}$ by performing 48 scans, with a resolution of $4\ cm^{-1}$. The software Opus® software (Bruker Optics, Germany) was used for data acquisition. The spectra were averaged, baseline corrected, and vector normalized using Thermo Nicolet's OMNIC 6.0 and Origin 9. From the processed spectra, the semi-quantification of selected bands was performed. Finally, the percentage of intensity variation of some bands was calculated using Eq. (2)[37]:

$$\Delta I\% = [(I_f - I_i)/I_i] \times 100\% \qquad (2)$$

I_i is the initial value of the intensity and I_f is the final value. In this study, FTIR-ATR provided information on the nature of the binding media and pigments, and indicated possible degradation phenomena over a wide time range. For this purpose, analyses were carried out on SET1 and SET2 samples every 4 h on the first day, every day for the first 2 weeks, once a week for the first month, then once a month until the seventh month.

GC-MS analyses were performed according to a procedure that has been successfully tested for modern and contemporary oil paints[15,18,38–41]. The GC-MS analysis was performed by using Thermo Scientific™ TRACE™ 1300 Series GC System equipped with an ISQ 7000 MS quadrupole analyzer by Thermo Fisher Scientific. Samples were autoinjected in splitless mode at 280 °C and GC separation was performed on a fused silica capillary column DB–5MS column (30 m length, 0.25 mm, 0.25 μm—5% phenylmethyl polysiloxane), using helium as the carrier gas (1 mL/min flow rate). The transfer line was at 280 °C and the MS source temperature was 300 °C. The temperature was programmed from 80 °C to 315 °C with a 10 °C ramp and held isothermally for 2 minutes; the total run time was 27.50 minutes. The volume injected was 1 μL and the solvent delay was set to 8 minutes. The MS scans were performed in full scan mode, covering the range from 40 to 650 m/z, at 1.9 scans/s. Electron Ionisation energy was 70 eV.

Data were processed using Chromeleon Chromatography Studio.

The compounds were identified as methyl esters (following a transesterification reaction) by comparison with the NIST library. The samples were prepared using the MethPrepII™ derivatizing agent, a methylesterifying agent consisting of a 5% solution of m(trifluoromethyl)phenyltrimethylammonium hydroxide in methanol. Quantitative analysis was performed using nonadecanoic acid as the internal standard and a standard solution containing saturated (myristic, palmitic, stearic, azelaic, suberic, sebacic) and unsaturated (oleic, linoleic, linolenic, palmitoleic) fatty acids and glycerol.

The molar ratios of the main fatty acids considered were: A/P (ratio of azelaic acid to palmitic acid) to distinguish drying oils from egg lipids; P/S (ratio of palmitic acid to stearic acid) conventionally used for the identification of conventional drying oil paints; A/Sub (ratio of azelaic acid to suberic acid) to provide an assessment of any preheating processes that may have occurred in the preparation of the oil; D/P (ratio of dicarboxylic acid to palmitic acid ratio) to provide an assessment of the degree of drying as di-fatty acids are more abundant in aged films; O/S (ratio of oleic acid to stearic acid ratio) can indicate the maturity of oils (i.e., the amount of unsaturated fatty acids remaining)[1,41,42]; D% (total percentage of dicarboxylic acid) to provide information on the degree of oxidation of the oil[11,43,44].

GC-MS analyses were performed on oil films from SET1, every 4 h on the first day, every day during the first 2 weeks, once a week during the first month, then, once a month until the seventh month after casting.

Based on the method used in previous research on contemporary oil films[45], the present study on oxidative degradation was extended to observe thermal behaviour.

A Netzsch 409/C apparatus was used, and the data were collected using STA Netzsch software and then processed using Origin 9 software. The crucible used as a reference consisted of an alumina standard. Samples were weighed in an aluminium crucible using the TG internal balance. Alumina was used for the internal calibration. The instrument was programmed for a temperature rise of 10 °C/min with a range between 30 °C and 1050 °C and an air flow of 40 mL/min.

The subject of investigation concerns paint layers containing organic and inorganic substances capable of undergoing chemical or physical transitions as the applied temperature changes. For this reason, the thermal behaviour and the oxidative stability of earth colours in SET1 were investigated. TG-DSC analyses were carried out on burnt Sienna, raw umber, raw Sienna, and burnt umber at 0 h (fresh paint), after four days (in the dry-to-the-touch phase), and after three months.

Results

For the sake of clarity, the results are presented grouped as follows: (1) cobalt blue, (2) earth colours (burnt umber, burnt Sienna, raw Sienna, red iron oxide, yellow ochre), and (3) white colours (zinc, titanium and lead white). This distinction was convenient as the oil paints within each group presented comparable results.

Scribe tests

As mentioned above, this is the first scientific study to correlate the results of a multi-analytical campaign with those obtained by scribe tests.
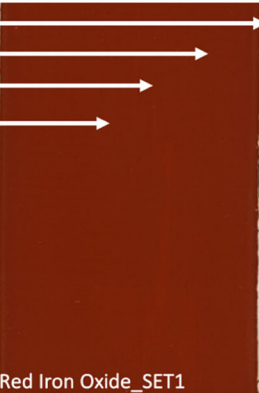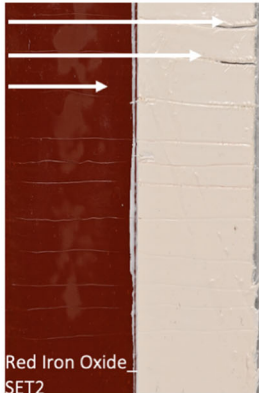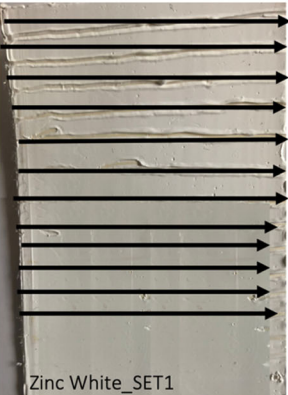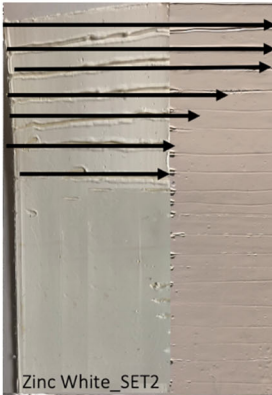
Scribe tests were carried out on the oil paint films studied from the very first moment after being cast until the paint film was dry-to-the-touch and the stick was no longer able to slide (Table 3). These tests made it possible to observe how long the paint films took to dry as a function of the pigment present in their composition but also how an adjacent white lead oil paint film could influence the drying process.

The role of pigments in drying was assessed: results showed that cobalt blue was dry-to-the-touch 24 h after casting, whereas earth colours required 48–72 h depending on the elemental composition of the earth pigments. Pigments containing manganese (such as raw and burnt umbers) dried after 48 h, whereas raw and burnt Sienna, red iron oxide, and yellow ochre took 72 h.

White paint films showed a different behaviour. Titanium white took 20 days for the stick to leave no trace on the paint film, while zinc white took 21 days. The test shows that selected auxiliary white metal ions (titanium and zinc) do not drive a catalytic reaction independently, as previous analyses have also shown. These metal ions show better drying properties only in combination with primary metal ions, activating the catalytic behaviour[46].

This can be interpreted, especially for zinc white, as a consequence of the formation of unsaturated fatty acids via other reaction pathways and a low presence of the already mentioned peroxyl radical reactions[47–49]. Zinc oxide, in particular, is known to create a structure that can trap unsaturated fatty acids, affecting the formation of the paint film, its stability, and the formation of degradation products such as protrusions[22,23,30,50].

Table 3 | Summary of the result obtained with the scribe test

GROUPS	SET 1 SINGLE LAYER PAINT FILM CAST IN 2021	SET 2 COLOR PAINT FILM NEXT TO LEAD WHITE PAINT FILM CAST IN 2021
1) COBALT BLUE	 1st day 2nd day: dry to touch Cobalt blue_SET1	 1st day 2nd day: dry to touch Cobalt blue_SET2
2) EARTH COLORS	 1st day 2nd day 3rd day 4th day 5th day: dry to touch Red Iron Oxide_SET1	 1st day 2nd day 3rd day 4th day: dry to touch Red Iron Oxide_SET2
3) WHITE COLORS	 1st day 2nd day 3rd day 4th day 5th day 6th day 7th day 8th day 9th day 10th day 11th day 12th day 13th day 14th day: dry to touch Zinc White_SET1	 1st day 2nd day 3rd day 4th day 5th day 6th day 7th day: dry to touch Zinc White_SET2

The tests were performed on samples of SET1 (Single-layer paint films) and SET2 (Side-by-side paint film) of: (1) cobalt blue; (2) earth colors; (3) whites colors; the arrows are positioned close to the slide; the tip of the arrow corresponds to the end of the mark observed on the surface.
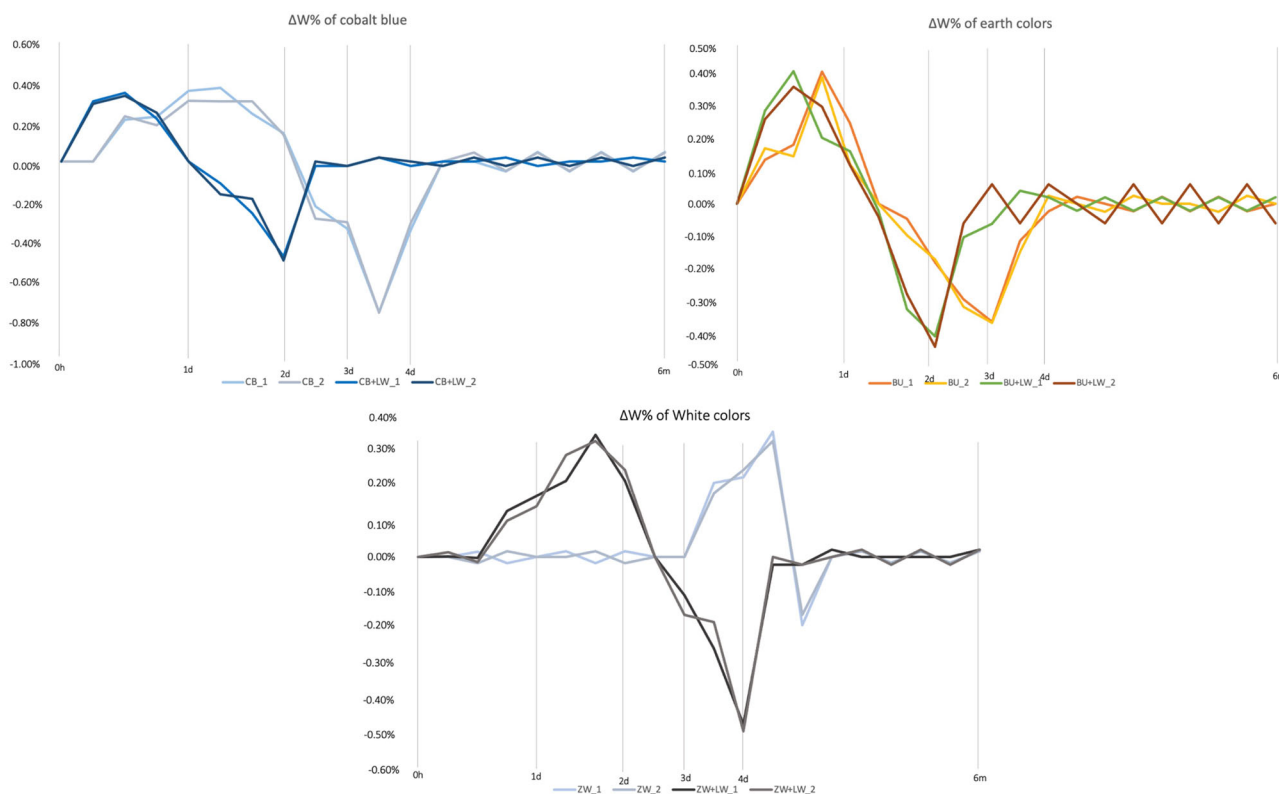
Fig. 2 | Percentage weight variation diagram. ΔW% of cobalt blue, earth colors, and white colors in SET1 and SET2 calculated using Eq. (1) every 4 h on the first day, every day during the first 2 weeks, once a week during the first month, once a month until the seventh month.

Table 4 | Summary of the main catalytic chemical reactions that occurred according to the percentage weight variation of cobalt blue, earth colours, and white colours in SET1 and SET2

Catalytic chemical reaction	Comment	TIME					
		Cobalt blue		Earth colours		White colours	
		SET 1	SET2	SET 1	SET2	SET 1	SET2
$RH + M^N \rightarrow R° + H^- + M^{N-1}$	During the initiation phase, metal ions can trigger a radical-chain reaction in which the metal changes its oxidation state through the transfer of electrons from a higher (M^N) to a lower (M^{N-1}) state. An increase in mass weight occurs due to the rapid initial absorption of large quantities of atmospheric oxygen.	4 h	0 h	6 h	0 h	3 d	12 h
$ROOH + M^N \rightarrow ROO° + H^- + M^{N-1}$ $ROOH + M^{N-1} \rightarrow RO° + OH^- + M^N$	These two simplified reactions provide a reduction-oxidation (redox) mechanism that can promote polymerization. A weight loss is observed related to the secondary cleavage reactions.	84 h	2 d	3 d	2 d	6 d	4 d

The column TIME displays when a specific catalytic chemical reaction occurred. h hours, d days, w week.

On the other hand, the scribe tests on SET2 samples showed what had been previously hypothesised: lead ions, migrating transversely into the adjacent paint film, are able to influence the autoxidation reaction of unsaturated lipids through a metal-catalysed reaction with the primary and auxiliary metal ions of the adjacent oil paint film[19–21]. This catalytic reaction is more pronounced for metal ions with less siccative properties. While cobalt (known to be the best catalyst for oxidative processes) does not seem to be particularly affected by the presence of lead white, earth colours were dry-to-touch 24 hours faster when in contact with lead white; the presence of lead also accelerated the drying of titanium white oil paint film, reducing its drying time to 14 days (half the drying time of titanium white alone), and that of zinc white to 7 days (1/3 of the time of zinc white alone)[29,31,51].

In addition, Mn-containing iron oxide pigments dried faster than those without Mn in SET 1: raw and burnt umber were dry-to-the-touch after 24 h; whereas, raw and burnt Sienna, red iron oxide and yellow ochre needed 48 h to be dry-to-the-touch. This confirms that some metals have more effective drying properties than others.

Comparing the results from SET 1 and SET 2 allowed observations to be made on the influence of lead white when applied next to a coloured paint film. The results of the scribe tests were fundamental in defining the time frame in which other repeated analyses (such as weight measurements and ATR-FTIR) were carried out in this study

Percentage weight variation

As shown in Fig. 2, the ΔW% analysis allowed the weight gain and loss of each paint film to be monitored at different times.

It is known that the weight increase in mass immediately after casting is related to the initial rapid absorption of large amounts of atmospheric oxygen, leading to the formation of peroxidic compounds[1]. It was interesting here to determine the different effects that certain metal ions had on

Table 5 | Summary of the main ATR-FTIR absorption changes over time of mockups in SET1 and SET2

Peak cm^{-1}	Assignment	TIME						Comment
		Cobalt blue		Earth colours		White colours		
		SET 1	SET 2	SET 1	SET 2	SET 1	SET 2	
3450	v (O-H)	24 h	24 h	24 h	24 h	48 h	24 h	Formation of a broadband characteristic of alcohol and hydroperoxide groups.
3008	v (C-H)	48 h	48 h	20d	10d	1w	7d	Decreasing intensity due to the unsaturated bond C = C-H; it is confirmed by the presence of a peak at 729 cm^{-1}, covered by the pigment in some cases.
2955	v (C-H$_3$)	72 h	72 h	96 h	48 h	96 h	72 h	Decreasing intensity of the peak.
1744	v(C = O)	1 m	1w	7w	2w	7 m	7w	Broadering of the ester stretching (C = O) band due to hydrolysis of triglycerides and the formation of other degradation products.
1713	v(C = O)	6 m	4 m	7 m	5 m	-	7 m	A small shoulder on the peak at 1740 cm^{-1} related to C = O stretching movements associated with free fatty acid formed by hydrolysis.
1623	δ (COO$^-$)	2 m	2 m	72 h	48 h	96 h	72 h	Increasing the intensity due to C = C stretching
1417-1427	v (C-O) Asymmetric	48 h	48 h	72 h	48 h	48 h	36 h	Formation of doublet due to CH$_2$ Wagging and COO- stretching of fatty acid.
1236,1182, 1098	v (C-O)	96 h	96 h	72 h	48 h	-	-	Increasing the intensity due to ester bonds (C-O).

The column TIME displays when a specific absorption was first observed. v stretching, δ deformations, h hours, d days, w week, m month.

the autoxidation of the drying oil, which was visible from the very first hours after casting (Table 4). In particular, this study showed that the absorption of oxygen started immediately in the cobalt blue and earth-coloured paint films, while it started after 3 days in the titanium and zinc paint films. The metal ions Co^{2+}, Mn^{2+}, and Fe^{2+} are, indeed, considered as "primary" driers and act as catalysts during oxidation. The ion Ti^{2+} is also in this category but it is the worst catalyst of the group, exhibiting a similar behaviour to Zn^{2+}, which is instead considered an auxiliary drier as it acts to modify the activity of the primary driers[1,17,26,44,52]. This again shows that some metals have better drying properties than others.

As drying progressed, the development of cross-links occured at a slower rate and the decrease in weight indicated that secondary cleavage reactions predominated over oxygen uptake[5,8,44]. The cleavage of alkoxy radicals from the peroxidation of unsaturated triglyceride fatty acids led to the formation of various molecules such as hydrocarbons, furans, and oxidised or hydroxylated fatty acids[1,11,40,53–56]. This second phase resulted in weight loss due to the decomposition of formed oxygen compounds (such as hydroperoxides) with the evolution of several relatively low molecular weight molecules, including several degradation products such as aldehydes and ketones[8,38,44,57].

The experimental data showed that the greatest weight loss in SET1 occurred within 3 days in the cobalt and earth oil paint films, with the reaction times of the manganese-containing earths (raw and burnt umber) being 24 h faster than the predominantly iron-containing earths (raw and burnt Sienna, iron oxide red and ochre yellow), as observed in the scribe test (Fig. 2).

It is well known that the metals with the most effective drying properties are cobalt and manganese, since the metals can exist in at least two valence states and are able to exert a catalytic effect on the autoxidation process; the highest valence is the least stable metal[1,5]. White colours behave differently: white titanium and zinc paint films take 10 days before reaching weight stability. Zinc oxide and titanium oxide take longer to stabilize because they react with the carboxyl groups formed during polymerisation reactions, resulting in metal ions binding to pendant carboxylate groups in the lipidic polymer network[19–21,31,50]. In this ionomeric state, zinc ions can further react with saturated fatty acids to form zinc soaps, which tend to separate from the polymeric medium[22,23,30,58].

Analysis on SET2 showed that the presence of lead white adjacent to a paint film accelerated the rate of the weight gain and subsequent weight loss, in particular, by 24 h in the case of cobalt blue and earth colours and by 48 h in the case of white colours. It has been shown that lead white accelerates the

absorption of oxygen: the lead white acts in both oxidation and polymerisation reactions of the lipid binder, not only from the surface and through the paint film, as was already known, but also by being in contact with the paint film[11,21,29,40,54].

Indeed, lead white is able to migrate into the adjacent paint film and catalyse the formation and/or decomposition of hydroperoxides formed by the reaction of oil with oxygen. The exact reaction of these ions with drying oils is not well understood but could be related to the concentration of saturated fatty soaps (possibly palmitic and stearic acids) and the binding capacity of each pigmented paint film. Lead ions are capable of accelearting the conversion of ROOH to RO° + OH, thereby triggering a double binding reaction[26,38–40] and affecting the forming properties of the adjacent paint film.

ATR-FTIR
ATR-FTIR analyses were carried out systematically over a long period of time (7 months) in order to understand the influence of the different pigments on the drying processes of the ARLO medium. Table 5 shows when spectral changes were detected after casting for each of the three groups mentioned above: (1) cobalt blue, (2) earth colours (burnt umber, burnt Sienna, raw Sienna, red iron oxide, yellow ochre), and (3) white colours (zinc, titanium and lead white).

Figure 3 shows the results of the semi-quantitative evaluation of selected bands: the percentage change in intensity of the C = C-H unsaturated bond at ~3008 cm^{-1}, the ester stretching (C = O) band at ~1744 cm^{-1} and the C = O stretching associated with free fatty acids at ~1713 cm^{-1}, are shown.

The most significant data are reported in this section, while all the analyses are presented in the supplementary material (Supplementary Figs. 1-10).

The IR data from SET1 confirmed the hierarchical drying properties of the primary drier present in cobalt blue and earth colours selected (Co>Mn>Fe), as widely reported in the literature[3,8–10,17,18,43]. The recorded spectra allowed to observe a difference in the drying behaviour of the earth colours as a broad band at ca. 3430 cm^{-1} (due to hydroxyl groups) and a weak absorption at 1633 cm^{-1} (related to the formation of conjugated double bonds) occurred 24 hours earlier in the predominantly manganese earth group than in the predominantly iron-containing earth group. The results therefore indicate how the enhanced catalytic effect of cobalt and manganese on the autoxidation process of the binder occurs[11,13,17,20,43,59–63]. In contrast, the spectra of the white group showed a lower occurrence of the above mentioned peroxyl radical reactions[20,21,48,58,64]: the broadening of the

Fig. 3 | Percentage variation in the intensity of selected bands in cobalt blue, burnt umber, and zinc white of SET1 and SET2 calculated using Eq. (2). The band considered are ν(C-H) at ~3008 cm^{-1}, ν(C = O) at ~1744 cm^{-1} and ν(C = O) associated with free fatty acid at ~1713 cm^{-1}. h hours, d days, w week, m month, 0% no variations are reported.
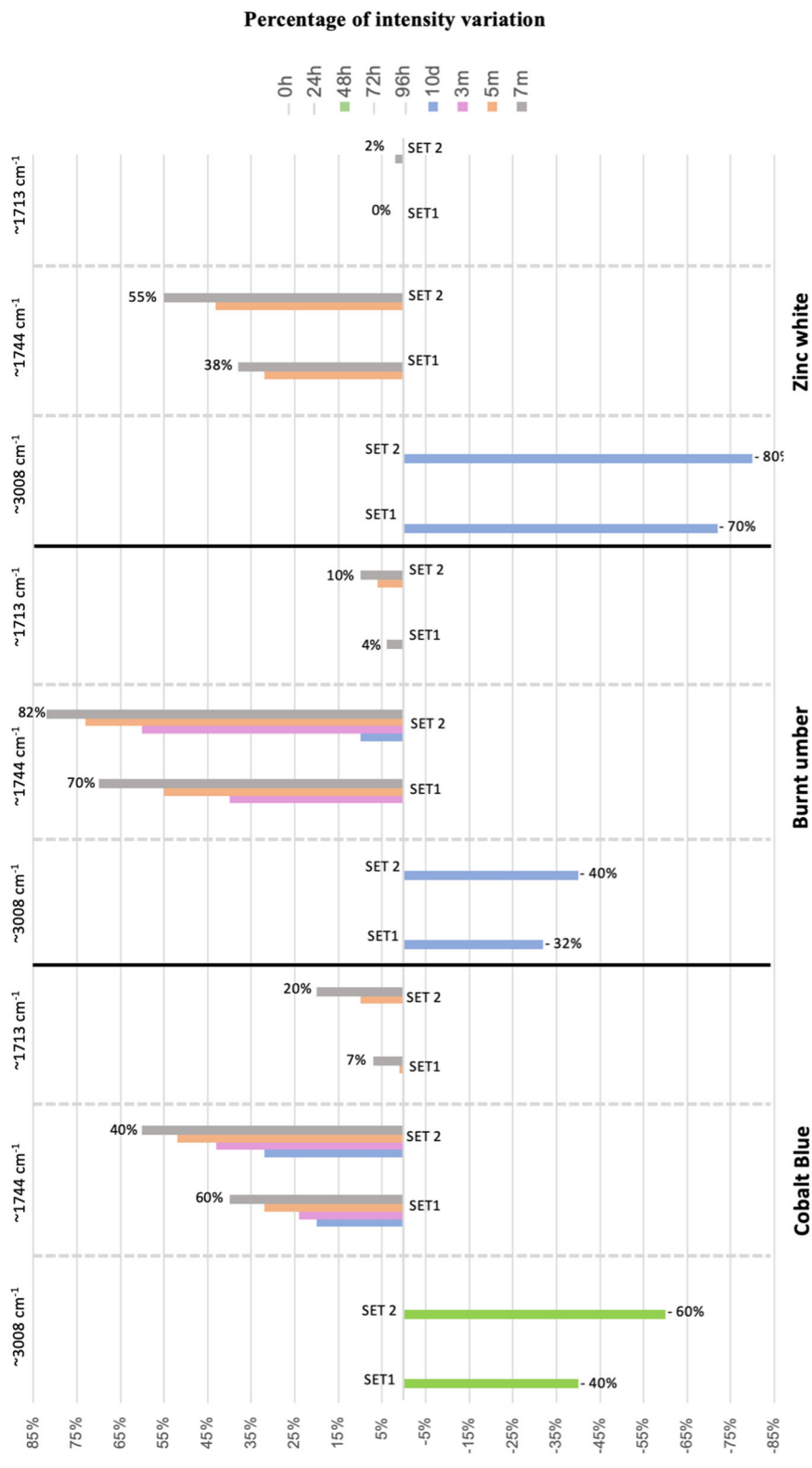
ester stretching band (C = O) is observed after 6 months compared to the spectra of cobalt blue and earth colours. The ester stretching band intensity at around 1744 cm^{-1} increased of 40% in cobalt blue, of 70% in burnt umber and 38% in zinc white after 7 months.

According to the results of the weight variation analysis, it was expected that the greatest structural changes would be observed in the first 4 days after casting, followed by the attainment of stability (Table 5).

The IR analysis, on the other hand, showed significant changes up to 10 days after casting, due to the hydrolysis of the triglycerides. In addition, while previous analyses have shown that the metal ions have a positive influence on the drying processes and subsequent stability of the paint film, IR spectroscopy also allowed the detection of possible degradation products (Fig. 4). Once free fatty acids have reacted with metal ions, they can lead to the formation of metal soaps, which can affect
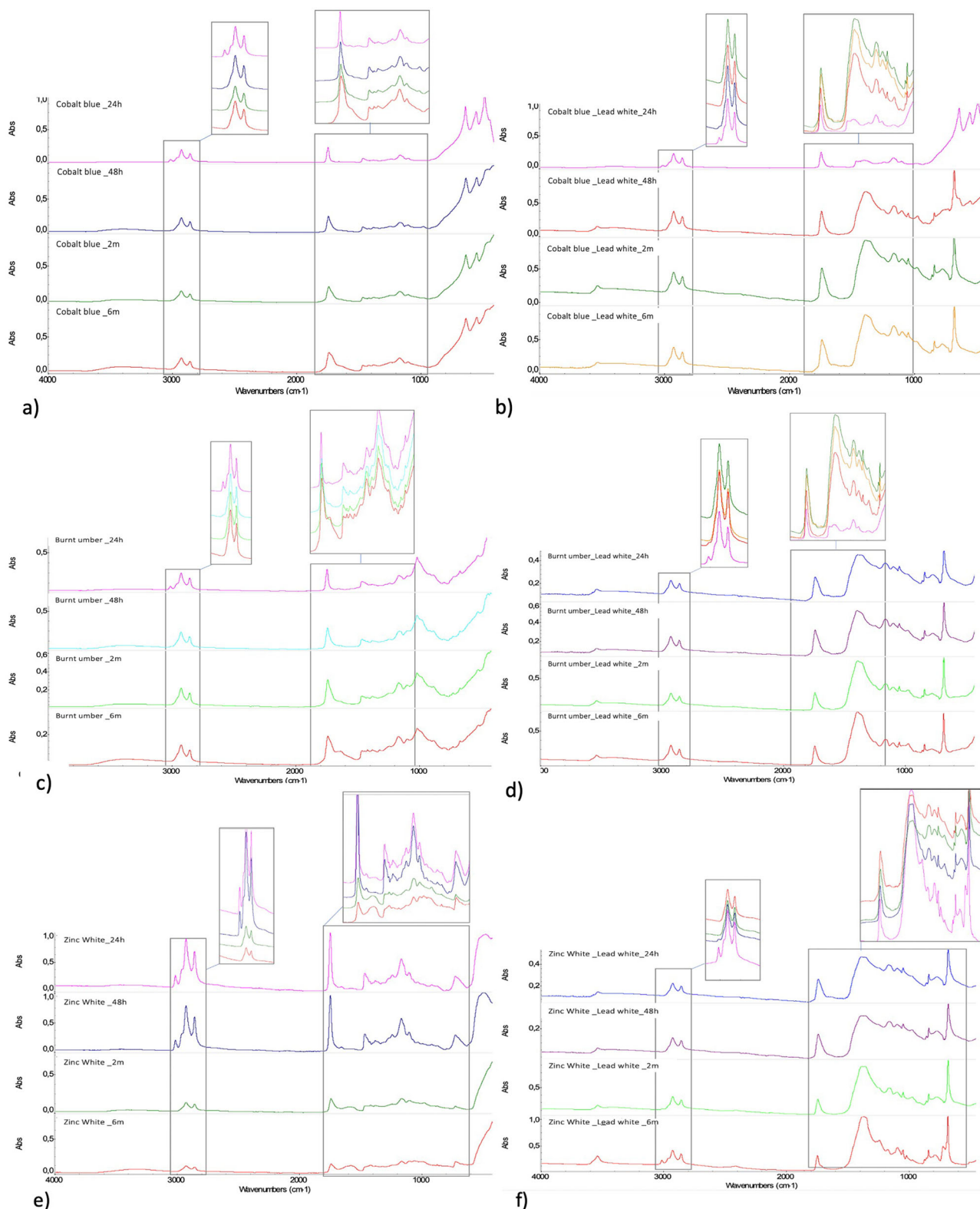
Fig. 4 | ATR-FTIR spectra. Analyses carried out after 24–48 h and 2–7 months of **a** Cobalt blue in SET1; **b** Cobalt blue with lead white in SET2; **c** Burnt umber in SET1 **d** Burnt umber with lead white in SET2; **e** Zinc white in SET1, **f** Zinc white with lead white in SET2.

the physical, chemical, and mechanical properties of paintings[65,66]. Metal soaps are generally responsible for many degradation processes (e.g. protrusions, efflorescence, and browning[6,12,13,15]). Metal soaps are also sometimes thought to play a positive role as anchoring points during the drying process of paintings[19].

As previous studies have shown, the formation of free fatty acids is generally visible one year after casting[47–49,60]. In this study, the corresponding peak at ~1713 cm^{-1} was observed in cobalt blue with a percentage change in the intensity of 7%. In raw and burnt umber it was observed 6 months after casting with an increasing of 4%. In the

Table 6 | Main changes of the TG-DSC curve at 0 hours, after 4 days, after 3 and 6 months of burnt umber, raw umber, burnt Sienna, raw Sienna

	Burnt umber			Raw umber			Burnt Sienna			Raw Sienna		
	Δ range (°C)	Δw%	ΔT (°C)	Δ range (°C)	Δw%	ΔT (°C)	Δ range (°C)	Δw%	ΔT (°C)	Δ range (°C)	Δw%	ΔT (°C)
0 hours	275-350	−7.08	315.1-Exo	350-400	−22.30	346.6-Exo	350-400	−18.58	332.9-Exo	350-400	−22.30	346.6-Exo
	350-400	−14.11	351.5-Exo	400-475	−10.80	473.0-Exo		−22.26	377.7-Exo	400-475	−10.80	473.0-Exo
	350-400	−27.18	398.0-				400-475	−11.53	485.7-Exo			
	475-525	−0.26	Endo				475-560		549.5			
	525-700		510.5-Exo									
			595- Endo									
4 days	50-150	−3.32	130.2- Exo	50-150	−6.75	131.7-Exo	50-150	−8.94	134.6-Exo	50-150	−5.56	133.8-Exo
	275-350	−16.84	319.1- Exo	350-400	−22.04	354-Exo	350-400	−11.57	349.2-Exo	275-350	−43.48	241.8-Exo
	350-400	−15.66	366.3- Exo	400-475	−18.68	439.4-Exo	400-475	−23.32	437-Exo	350-400		323.4-Exo
	400-475	−13.42	442.8- Exo	475-525	−18.04	457.9-Exo	475-525	−1.44	464-Exo			377.9-Exo
	475-525	−0.08	511- Exo	625-700		524-Endo				400-475		443.5-Endo
	625-700		589.8 -Exo							475-525		519.8-Exo
										625-700		779.4-Endo
3 months	50-150	−6.6	137.5- Exo	50-150	−46.76	133.2-Exo	50-150	−22.24	143.1-Exo	50-150	−23.38	144.6-Exo
	300-400	−36.9	333.7- Exo	275-350	−18.11	341.7-Exo	350-400	−12.7	339.5-Endo	350-400	−8.81	338.6-Exo
		−5.43	380.7- Exo	350-400	−0.80			−15.82	431.7-Endo		−13.93	367.5-Exo
	430-525	−0.48	439.9- Exo	625-700		432.0-Exo	475-525	−1.20	501.1-Exo	400-475		441.5-Exo
	525-700		595.4- Endo	400-475		466.1-Exo	625-700		739.7-Endo	475-525		494.0-Exo
				475-545		541 Endo						
6 months	50-150	−10.7	41.0- Endo	50-150	−11.44	41.6-Endo	50-150	−18.70	41.0-Endo	50-150	−5.33	40.9- Endo
		−34.53	168.3-Endo		−30.28	131.7-Exo	230-350	−38.32	238.9-Exo	250-400	−20.21	275.7-Exo
	350-400	−10.68		350-400	−7.46	320.7-Exo	350-400		377.5-Exo	420-525	−17.31	391.1-Exo
	400-600	−42.38	242.1- Exo								−4.41	441.0-Exo
		−0.55	377.5-Exo	420-525		424.4-Exo	450-700		482.3-Exo	550-700		494.2-Exo
			48.3-Endo			471.6-Exo			546.6-Exo			521.1-Exo
			546.9- Exo	550-700		589.4-Exo						600.2-Exo

Exo Exothermic reaction, *Endo* Endothermic reaction, Δ *range (°C)* Range of variation in °C; Δ*w*% Percentage weight loss, Δ*T (°C)* Temperature of variation.

case of raw and burnt Sienna, iron oxide red and ochre yellow the peak was observed 7 months after casting.

The absence of additives declared by Golden, the manufacturer, highlights the role of metal ions not only in the formation of the paint film but also in the degradation products released. This study proved that:

cobalt blue and earth colours accelerate the formation of free fatty acids and the resulting metal soaps;

no peaks related to free fatty acids are observed in white colours, being consistent with what has been reported in the literature[6,14,48].

The IR spectra of SET2 showed the catalytic action of lead white in the formation of metal soaps and their transversal migration. The cobalt and earth colour spectra of SET2 showed that the peak at ~1713 cm⁻¹ is visible 4 and 5 months after casting andincreased by 20% and 10% respectively after 7 months. This indicates that in SET 2 samples, the formation of free fatty acids occurred 2 months earlier than in the SET 1 samples. The presence of free fatty acids observed in the spectra of the white colours (zinc and titanium side-by-side with lead white) in SET 2 after 7 months (increase of 2%) shows that lead ions have migrated transversely into the adjacent burnt umber oil paint film by accelerating the unsaturated lipid autoxidation

reactions through a catalytic reaction with the auxiliary metal ions of the earth pigment.

TG-DSC

Given that the ATR-FTIR results suggested a role for the earth colours in the oxidation and hydrolysis reaction pathway of the triglycerides, it was essential to also understand the thermal behaviour and the oxidative stability of the oil films over time.

The TG curves of fresh oil earth colours show a first mass loss between 250 and 400 °C followed by a second above 400 °C (Table 6). This first loss is related to the oxidative decomposition of oxygen-rich compounds and the volatilisation of organic fractions (decomposition products), as reported in the literature[11,43,44]. DSC analysis generally shows two exothermic peaks around 380 and 430 °C related to oxidative degradation.

After 4 days, a slight mass loss can be observed at 150 °C, related to the decomposition of hydroperoxide groups with the formation of radicals that react with C = C, leading to an exothermic cross-linking process. According to the literature, these processes are visible after 1 year, whereas in the samples analyzed, the peak related to the decomposition of hydroperoxides is already visible after 4 days[45,53]. This faster degradation might be due to the

Table 7 | List of compounds identified by GC-MS and their concentration calculated in μg/mg

Identified Compound	m/z	Zinc white									Lead white								
		8 h	24 h	72 h	1w	2w	4w	15w	22w	7 m	8 h	24 h	72 h	1w	2w	4w	15w	22w	7 m
Fatty acid and other compounds																			
Octanoic acid ME	144	n.d.	n.d.	n.d.	n.d.	✓	✓	✓	✓	✓	n.d.	n.d.	n.d.	n.d.	✓	✓	✓	✓	✓
Glycerol derivate	89	✓	✓	✓	✓	✓	✓	✓	✓	✓	✓	✓	✓	✓	✓	✓	✓	✓	✓
Glycerol derivate	162	✓	✓	✓	✓	✓	✓	✓	✓	✓	✓	✓	✓	✓	✓	✓	✓	✓	✓
Nonanoic acid, 9-oxo ME	172	n.d.	n.d.	n.d.	n.d.	✓	✓	✓	✓	✓	n.d.	n.d.	n.d.	n.d.	✓	✓	✓	✓	✓
Suberic acid diME	202	n.d.	n.d.	n.d.	0.65	0.89	1.73	2.37	68	8.58	n.d.	n.d.	n.d.	0.81	1.30	2.37	4.33	14.78	15.07
Glycerol derivate	75	✓	✓	✓	✓	✓	✓	✓	✓	✓	✓	✓	✓	✓	✓	✓	✓	✓	✓
Decanoic acid, 9-oxo-ME	200	n.d.	n.d.	n.d.	n.d.	✓	✓	✓	✓	✓	n.d.	n.d.	n.d.	n.d.	✓	✓	✓	✓	✓
Azelaic acid diME	216	0.33	0.36	1.44	8.65	10.02	11.95	14.21	26.87	33.84	0.17	0.52	1.69	9.99	10.79	13.75	19.21	36.87	36.98
Sebacic acid diME	230	n.d.	n.d.	n.d.	0.57	0.7	0.7	0.82	2.86	2.91	n.d.	n.d.	n.d.	0.66	0.69	0.88	0.89	3.57	4.67
Myristic acid ME	242	✓	✓	✓	✓	✓	✓	✓	✓	✓	✓	✓	✓	✓	✓	✓	✓	✓	✓
Glycerol derivate	394	✓	✓	✓	✓	✓	✓	✓	✓	✓	✓	✓	✓	✓	✓	✓	✓	✓	✓
Palmitoleic acid	268	✓	✓	✓	n.d.	✓	✓	✓	✓	✓	✓	✓	✓	n.d.	✓	✓	✓	✓	✓
Palmitic acid ME	270	9.89	12.62	12.62	12.57	12.86	14.21	10.25	12.06	12.07	12.86	11.81	10.13	13.55	13.47	14.78	14.79	13.04	13.87
Linoleic acid ME	292	18.29	17.99	17.53	8.86	3.21	0.57	n.d.	n.d.	n.d.	7.30	2.33	1.49	0.39	n.d.	n.d.	n.d.	n.d.	n.d.
Oleic acid ME	296	30.02	27.15	15.1	0.86	4.92	1.51	0.73	0.55	0.46	27.94	24.78	23.32	19.39	18.72	17.22	1.03	0.72	0.13
Stearic acid ME	298	10.52	11.84	10.6	10.53	10.37	11.22	10.38	11.67	9.39	11.75	10.06	10.00	9.94	9.99	9.97	10.4	11.01	10.13
Linolenic acid ME	294	7.17	4.85	1.89	1.17	1.34	1.04	0.57	n.d.	n.d.	1.02	1.13	1.13	1.20	0.28	N.D.	n.d.	n.d.	n.d.
Nonadecanoic acid ME	312	✓	✓	✓	✓	✓	✓	✓	✓	✓	✓	✓	✓	✓	✓	✓	✓	✓	✓
Octadecanoic acid, 9,10-epoxy ME	312	n.d.	n.d.	n.d.	n.d.	n.d.	n.d.	✓	✓	✓	n.d.	n.d.	n.d.	n.d.	✓	✓	✓	✓	✓
Eicosanoic acid ME	326	n.d.	n.d.	✓	✓	✓	✓	✓	✓	✓	n.d.	✓	✓	✓	✓	✓	✓	✓	✓
Glycerol main	134	✓	✓	✓	✓	✓	✓	✓	✓	✓	✓	✓	✓	✓	✓	✓	✓	✓	✓
Arachidic acid ME	312	n.d.	n.d.	n.d.	n.d.	n.d.	n.d.	✓	✓	✓	n.d.	n.d.	n.d.	n.d.	n.d.	n.d.	n.d.	n.d.	✓
Octadecanoic acid, 9,10-dihydroxy ME	330	n.d.	n.d.	n.d.	n.d.	n.d.	n.d.	n.d.	n.d.	✓	n.d.	n.d.	n.d.	n.d.	n.d.	n.d.	n.d.	n.d.	✓
10-Octadecenoic acid ME	282	n.d.	n.d.	n.d.	n.d.	n.d.	✓	✓	✓	✓	n.d.	n.d.	n.d.	n.d.	n.d.	✓	✓	✓	✓
Behenic acid ME	340	n.d.	n.d.	n.d.	n.d.	n.d.	n.d.	✓	✓	✓	n.d.	n.d.	n.d.	n.d.	n.d.	n.d.	✓	✓	✓
Octadecanoic acid, 9,10-oxo- ME	310	n.d.	n.d.	n.d.	n.d.	n.d.	n.d.	n.d.	n.d.	✓	n.d.	n.d.	n.d.	n.d.	n.d.	n.d.	n.d.	n.d.	✓

Table 7 (continued) | List of compounds identified by GC-MS and their concentration calculated in µg/mg

Identified Compound	m/z	Zinc white									Lead white								
		8 h	24 h	72 h	1w	2w	4w	15w	22w	7 m	8 h	24 h	72 h	1w	2w	4w	15w	22w	7 m
Sebacic acid diME	230	n.d.	n.d.	n.d.	0.57	0.7	0.7	0.82	2.86	2.91	n.d.	n.d.	n.d.	0.66	0.69	0.88	0.89	3.57	4.67
Myristic acid ME	242	√	√	√	√	√	√	√	√	√	√	√	√	√	√	√	√	√	√
Glycerol derivate	394	√	√	√	√	√	√	√	√	√	√	√	√	√	√	√	√	√	√
Palmitoleic acid	268	√	√	√	n.d.	√	√	√	√	√	√	√	√	n.d.	√	√	√	√	√
Palmitic acid ME	270	9.89	12.62	12.62	12.57	12.86	14.21	10.25	12.06	12.07	12.86	11.81	10.13	13.55	13.47	14.78	14.79	13.04	13.87
Linoleic acid ME	292	18.29	17.99	17.53	8.86	3.21	0.57	n.d.	n.d.	n.d.	7.30	2.33	1.49	0.39	n.d.	n.d.	n.d.	n.d.	n.d.
Oleic acid ME	296	50.02	47.15	15.1	0.86	4.92	1.51	0.73	0.55	0.46	27.94	24.78	23.32	19.39	18.72	17.22	1.03	0.72	0.13
Stearic acid ME	298	10.52	11.84	10.6	10.53	10.37	11.22	10.38	11.67	9.39	11.75	10.06	10.00	9.94	9.99	9.97	10.4	11.01	10.13
Linolenic acid ME	294	7.17	4.85	1.89	1.17	1.34	1.04	0.57	n.d.	n.d.	1.02	1.13	1.13	1.20	0.28	n.d.	n.d.	n.d.	n.d.
Nonadecanoic acid ME	312	√	√	√	√	√	√	√	√	√	√	√	√	√	√	√	√	√	√
Octadecanoic acid, 9,10-epoxy ME	312	n.d.	n.d.	n.d.	n.d.	n.d.	n.d.	n.d.	√	√	n.d.	n.d.	n.d.	n.d.	√	√	n.d.	√	√
Eicosanoic acid ME	326	n.d.	n.d.	n.d.	n.d.	√	√	√	√	√	n.d.	n.d.	n.d.	√	√	√	√	√	√
Glycerol main	134	√	√	√	√	√	√	√	√	√	√	√	√	√	√	√	√	√	√
Arachidic acid ME	312	n.d.	n.d.	n.d.	n.d.	n.d.	n.d.	√	√	√	n.d.	n.d.	n.d.	n.d.	n.d.	n.d.	√	√	√
Octadecanoic acid, 9,10-dihydroxy ME	330	n.d.	n.d.	n.d.	n.d.	n.d.	n.d.	n.d.	n.d.	√	n.d.	n.d.	n.d.	n.d.	n.d.	√	n.d.	√	√
10-Octadecenoic acid ME	282	n.d.	n.d.	n.d.	n.d.	n.d.	n.d.	√	√	√	n.d.	n.d.	n.d.	n.d.	n.d.	√	√	√	√
Behenic acid ME	340	n.d.	n.d.	n.d.	n.d.	n.d.	n.d.	√	√	√	n.d.	n.d.	n.d.	n.d.	n.d.	n.d.	√	√	√
Octadecanoic acid, 9,10-oxo- ME	310	n.d.	n.d.	n.d.	n.d.	n.d.	n.d.	n.d.	√	√	n.d.	n.d.	n.d.	n.d.	n.d.	n.d.	n.d.	n.d.	√

The reported results were calculated by the chromatograms of cobalt blue, burnt umber, zinc white, and lead white mockups of SET1. *ME* methyl ester, *diME* dimethyl ester, *m/z* molecular weight of the most abundant mass fragment, *h* hours, *w* week, *m* month; √ present, *n.d* not detected, *h* hours, *d* days, *w* week, *m* month.
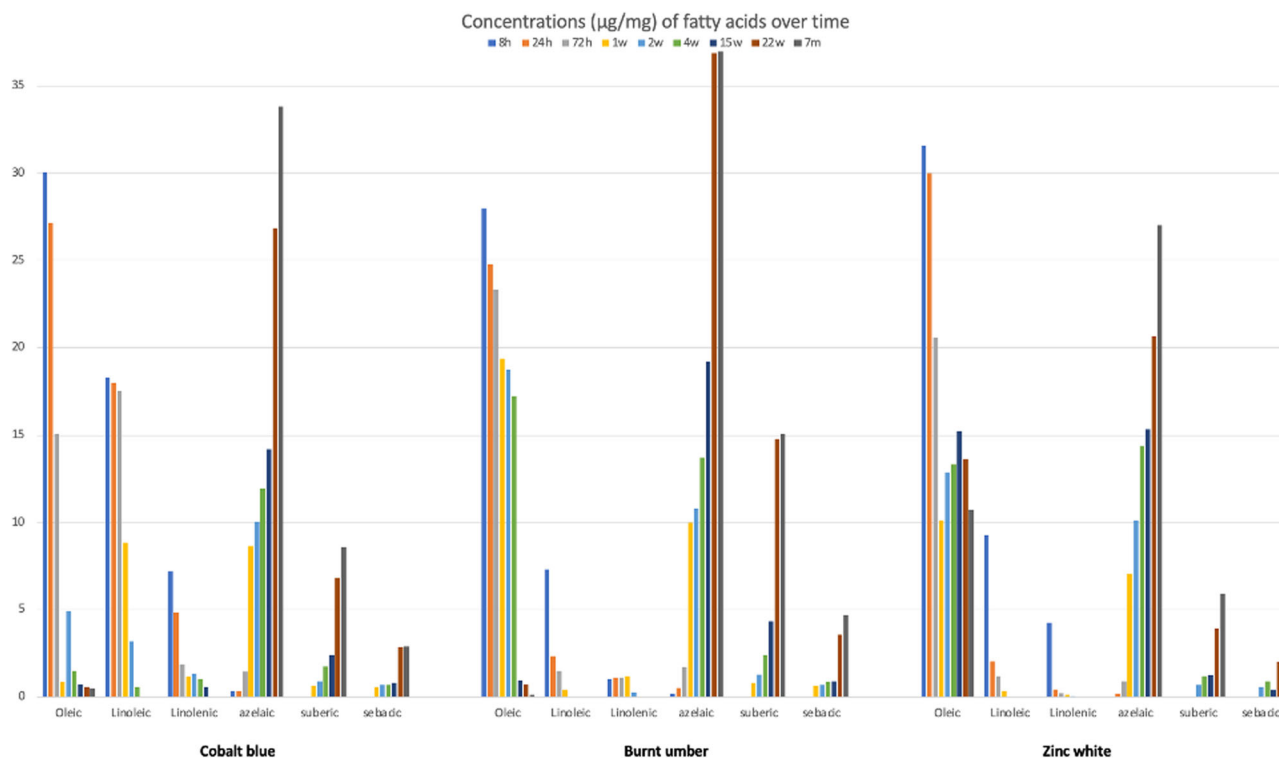
Fig. 5 | The graphic representation made with a 2D histogram of the variation over time (from time 8 hours to 7 months) of the concentrations (µg/mg) of fatty acids (sebacic, azelaic, suberic, linolenic, linoleic, oleic acids) in the SET1 of cobalt blue, burnt umber and zinc white. The increasing trend of saturated fatty acids and the decreasing trend of unsaturated fatty acids are shown. h hours, d days, w week, m month.

absence of additives in the selected paint systems by Golden Artist Colours (Figure S11-14).

It has been reported in the literature that the peak at 150 °C changes its amplitude over time due to the decrease in hydroperoxide concentration[67]. In the samples analysed after 6 months, it is indeed possible to observe that the peak is less resolved and broader compared to the curves observed after 4 days and 3 months. Moreover, after 6 months a well-defined peak appears at 546 °C, determined by the transformation of pyrolusite (MnO_2) into Mn_2O_3 (kurnakite)[11,45,53,65]. The mass loss is apparently due to the decomposition of the oxygen compound, as observed by monitoring the percentage change in weight. Active species such as peroxides and free radicals were detected after almost four days. This indicates a catalytic effect of the earth pigments also on the cross-linking mechanism.

GC-MS

GC-MS analyses were performed on the lipid fraction of the paint films from 8 h (fresh paint films) to 7 months after casting. The TIC (total ion current) chromatograms show all the characteristic fatty acids (as methyl esters) present in cured paint films (Figures S.15-24 and Tables S.1-S2). This allowed the identification of fatty acids and various oxidation, poly-merisation, and degradation products formed during the drying and curing processes of the ARLO pigmented films (Table 7).

The chromatographic data (Fig. 5) show a progressive decrease in the concentration of long chain unsaturated fatty acids (UFAs), such as oleic (C18:1), linoleic (C18:2), and linolenic (C18:3) over time, as expected for drying oils[8–11] (Table 7). Also in this case, the role of the pigments is clear: UFAs are not detectable after 1 week in cobalt blue (oleic acid concentration varied from ~50.2 µg/mg at 8 hours to ~0.8 µg/mg after 1 week), after 15 weeks in earth colours, after 7 months in the titanium colours (oleic acid concentration varied from ~34.32 µg/mg at 8 hours to ~0.49 µg/mg after 7 months), and after 22 weeks in lead white (oleic acid concentration varied from ~19.97 µg/mg at 8 hours to ~0.32 µg/mg after 22 weeks).

However, only in one case, that of the ZnO paint film, was a higher concentration of oleic acid was found, even 7 months after casting, despite ageing (i.e. a high degree of oxidation). In general, this phenomenon is most likely a consequence of the type of drying oil, but it can be explained differently when zinc oxide is present[1,8,11,12,14,20,44,53–56,58,64,68]. Zinc tends to form a packed structure that can trap oleic acid, thus forming zinc soap. This information is very important with regard to the degradation and stability of paint films: zinc soaps are generally associated with specific degradation phenomena, such as delamination, flaking and film splitting, thus com-promising the mechanical properties of paints[22,23,30].

Furthermore, after the oxidation of UFAs occurred, di-carboxylic fatty acids (SFAs), such as myristic (C14), palmitic (C16), and stearic (C18) were more clearly visible in the chromatograms. These SFAs, present in fresh linseed oil, are considered rather stable. However, as Schilling et al. have shown, there are minor differences: the amount of C16 and C18 saturated fatty acids can decrease unequally with exposure to light and due to the formation of metal soaps[1]. The standard deviation of palmitic and stearic acids are given in the supplementary material (Supplementary Table 2).

Dicarboxylic acids, typical tertiary oxidation products of unsaturated fatty acids, have been increasingly detected over time, in particular suberic (2C8), azelaic (2C9), and sebacic (2C10) acids. They are the main product of oxidative degradation and are formed as a consequence of fragmentations of triglycerides occurring in the cross-linked network. After 8 hours the per-centage of dicarboxylic acids (%D: suberic, azelaic, and sebacic acids) is ~0.8% and after 7 months it is ~40% of the total amount of fatty acids considered.

The numerous and abundant oxidised octadecanoic acids (oxo-, hydroxy-, and methoxy-octadecanoic acids) were produced by the oxidative cleavage of unsaturated fatty acids. They were detected after 1 week in cobalt blue, between 4 and 15 weeks in earth paint films, and after 7 months in white samples. Glycerol, considered as the sum of all its derivatives, was also detected as well in all paint films, both in fresh and cured paints. The molar ratios for azelaic/palmitic, palmitic/stearic, and azelaic/suberic allowed for
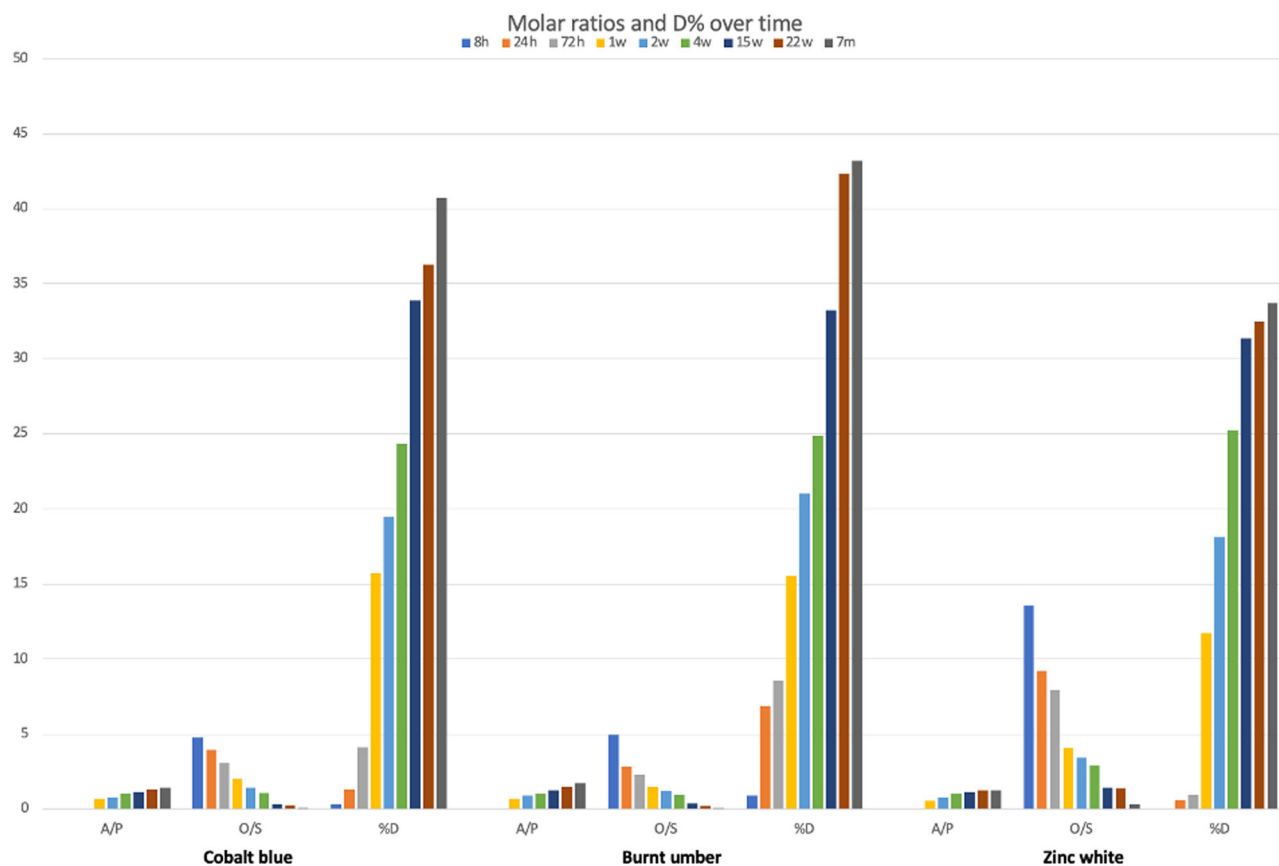
Fig. 6 | The graphic representation made with a 2D histogram of the variation over time (from time 8 hours to 7 months) of molar ratio (A/P, O/S) and %D in the SET1 of cobalt blue, burnt umber, and zinc white. The graphic representation made with a 2D histogram of the variation over time (from time 8 hours to 7 months) of molar ratio (A/P, O/S) and %D in the SET1 of cobalt blue, burnt umber, and zinc white. The increasing trend of %D, D/P, A/P and the decreasing trend of O/S molar ratio are shown. *A/P* (azelaic/palmitic); *O/S* (oleic/stearic); %D= (sum of the percentages of the following dicarboxylic acids: suberic, azelaic and sebacic); h hours, d days,w week, m month.

qualitative considerations: the use of a drying oil (A/P > 1), identified as linseed oil (P/S = 1.6), not preheated (A/Sub>6), was confirmed. This finding is consistent with the statement made by Golden Artist Colours regarding the use of ARLO in their formulations. In Fig. 6, the graphical representation of the molar ratio (A/P, O/S) and %D) over time shows the progressive decrease in the O/S ratio and the subsequent increase in the %D and dicarboxylic/palmitic molar ratios, suggesting that the samples experienced a significant oxidation rate after the first week.

Discussion

The methodology presented in this study provided information on early drying, oxidative polymerisation, and the formation of degradation products over time of selected custom-made oil paints (Fig. 6). A multi-analytical method determined the film forming process of each paint pairing as a function of the pigment present in the formulation and showed the migration of lead ions in side-by-side oil paint systems.

In this study, scribe tests provided observations of the time taken for selected oil paint films to dry-to-the-touch. The cobalt blue paint films dried the fastest of the single paint films observed (2 days, instead of the 5 days observed for the earth oil paint films). However, when two oil paint films were cast side by side, some differences were observed. For example, oil paint films containing earth pigments dried 24 h earlier when cast next to lead white oil paint films than when cast alone. In such cases, the hierarchical siccative properties also influenced the drying times observed (e.g. manganese-based paint films dried faster than yellow ochre and red iron oxide films). The drying speed of the titanium and zinc oil paint films also increased significantly when cast next to a white lead oil paint film, reducing the drying time to 14 days. This confirms that the presence of lead white

increases the rate of oxygen uptake, promotes drying, and improves the stability of the paint film when in contact with a primary drier (cobalt, manganese, iron, and titanium ions).

In order to determine the interaction taking place between pigment and binding media over time for each specific oil paint studied, the percentage weight change was monitored. The results obtained were of the utmost relevance, showing that the greatest changes in weight occurred in the first 4 days after casting for the oil paint films containing cobalt and earth colours, and in 10 days for the white oil paint films. It was also observed that the presence of lead white next to the samples accelerated the increase and subsequent loss of weight. This phenomenon was particularly evident in the titanium and zinc oil paint films where the weight change was significantly faster than when such paint films dried alone.

More detailed analyses were then carried out using spectroscopic, thermal, and chromatographic techniques in order to assess surface and bulk comparisons of the behaviour of metal ions in the lipid medium. ATR-FTIR spectra confirmed that the samples in SET2 retained their drying properties even when they were next to lead white. It was also confirmed that lead white increased the rate of oxygen uptake, thereby promoting the film formation processes and the formation of degradation products. These results confirmed that earth colours and cobalt blue had the fastest film forming reactions. The free fatty acid bands were more intense in the spectra of these paint films than in the other samples. This may indicate that cobalt and manganese play a role in the hydrolysis reaction pathway of the triglycerides. In addition, the alkali refining of linseed oil is very effective in the production of ARLO, a less impure oil (as mucilages and other impurities are generally washed out), but it requires the addition of a certain amount of free fatty acids in the drying oil to improve the wetting properties of the
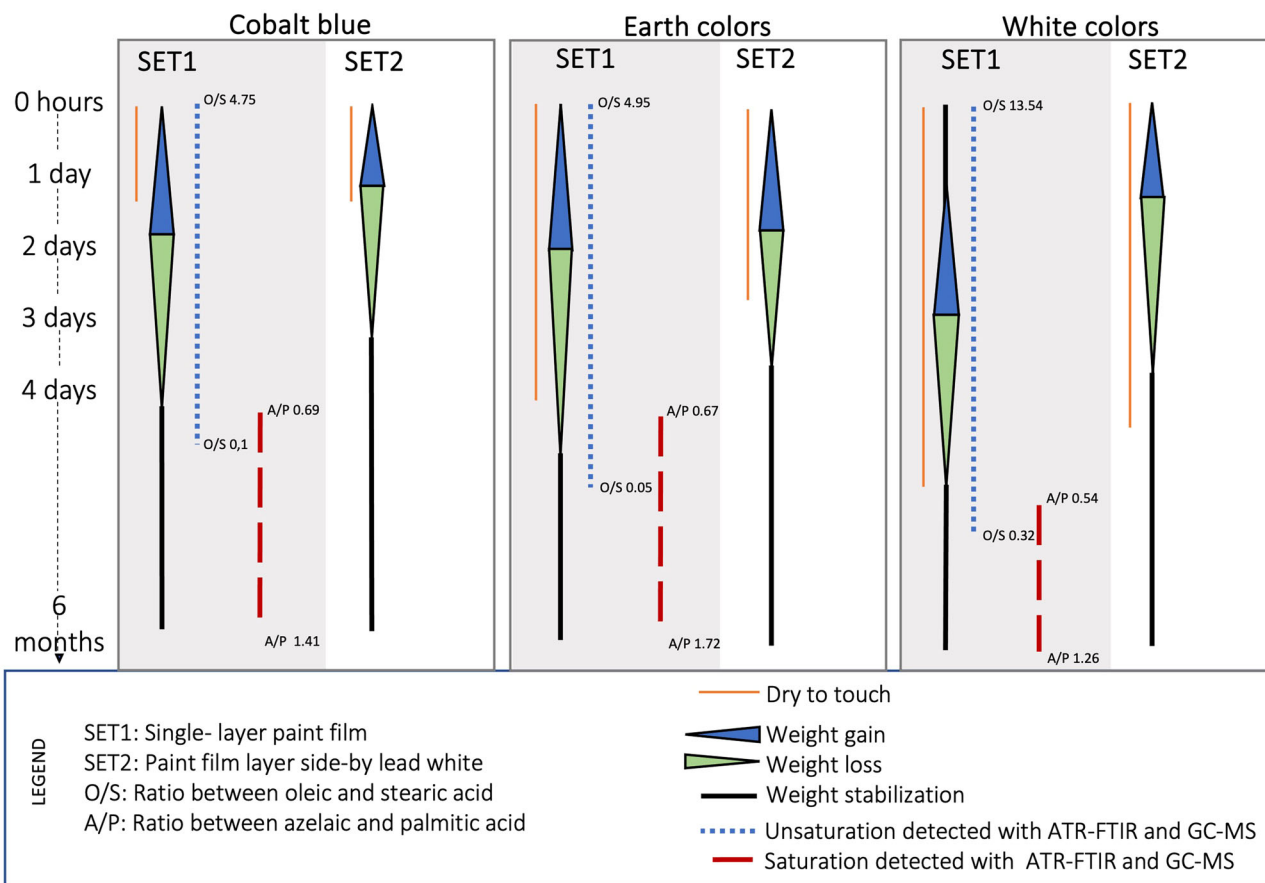
Fig. 7 | Summary of main results. The scribe test, weight percentage change, ATR-FTIR and GC-MS were compared to better visualize the final considerations in SET1 and SET2 of the colors cobalt blue, earth and white.

pigments in the final formulation[33]. These added free fatty acids may have enhanced the formation of metal soaps in the analysed paint films.

More detailed analyses of the thermal behaviour and oxidative stability of single-layer, earth paint films were carried out. TG-DSC curves of fresh samples showed the oxidative decomposition of oxygen-rich compounds and the volatilisation of organic fractions. After 4 days, peaks related to the decomposition of hydroperoxides with the formation of free radicals reacting with C = C could be observed. After 3 months, it was indeed possible to observe the peak related to the initial high concentration of hydroperoxides due to self-oxidation processes. The loss of mass due to oxidative degradation was observed by monitoring the percentage change in weight. Active species such as peroxides and free radicals were detected after almost four days. This indicates a catalytic effect of the earth pigments on the cross-linking.

In order to fully characterize the organic lipid fraction and to understand the effect of the ageing conditions on the paint films, GC-MS analysis was carried out over a wide time range. The comparison with the chromatographic analysis confirmed that the unsaturated fatty acids showed a progressive decrease in concentration after 1 week in cobalt blue, after 15 weeks in earth colours, and after more than 15 weeks in white colours. The O/S molar ratio of the white samples (zinc, titanium and lead white) confirmed the higher amount of unsaturation within the first month compared to the unsaturations of other colours. The progressive increase of dicarboxylic acids over time suggests that the oxidation process is taking place. The hypothesis is also confirmed by the numerous and abundant oxidised octadecanoic acids (oxo-, hydroxy-, and methoxy-octadecanoic) present after 1 week in cobalt blue, between 4 and 15 weeks in earth paint films and after 7 months in the white samples.

This study has enabled the interactions taking place between oil and pigment and between pigments in a paint film to be monitored from the first

hour after casting until the degradation of the material over a longer period and revealed how long they took to be dry-to-the-touch as a function of the pigment present and how the presence of a lead white oil paint film affected such drying and degradation products. More specifically, the multi-analytical approach made it possible to observe the interactions of metal ions with the oil binder (Fig. 7). Ions, such as lead, are capable of promoting both oxidation and polymerization of the oil, migrating transversely into the adjacent pictorial film and influencing its drying through a catalytic reaction capable of accelerating the autoxidation reactions of unsaturated lipids.

The results showed that the effect of lead white on the reactivity of polyunsaturated triglyceride fatty acids was pigment-dependent, i.e., in paint layers containing earth or cobalt blue pigments (made from primary metal ions), oxidative reactions increased more rapidly. This could be related to the presence of metal soaps formed by the reaction between metal ions and free fatty acids. In this regard, it could be interesting to evaluate how the percentage of fatty acids, depending on the type of oil, could influence the interaction of the medium with metal ions and the possible subsequent formation of metal soaps and other degradation products.

The most important aspect of the present study is the fact that unravelling and sequencing the factors that influence the physico-chemical mechanisms that take place in the early stages of film formation, curing and degradation of oil paint films, it is possible to design informed accurate conservation strategies to mitigate such degradation. For example, a recent study published as part of the MIMO project looks at how the results from laboratory experiments can be used to inform decisions in conservation practice. The paper provides an insight into how the study of pigment-medium interactions which take place mainly in the white areas has influenced the film formation, ageing and degradation observed in the Neo-Plasticist painting *Composition dans le cône avec couleur orange* by G. Vantongerloo (1929), which is kept at the Institut Valencià d'Art Modern (IVAM)[24]. The results of this research showed that the

degradation phenomena observed were closely related to the chemical composition of the painting materials, in particular to the interaction between the white pigments and the oil binding media, and not related to the environment. Such findings suggest that future studies should further explore the application of the methodology proposed in this study to evaluate the interaction between metal ions in pigments and other types of binders. For example, the potential migration of surfactants from polymeric binders in aqueous dispersions is currently being investigated. Initial results show that the surfactants wet the paint surface, making it more prone to attract dirt and dust, and thus more susceptible to react with pollutants. A better understanding of these mechanisms could also lead to better products for modern paints and coatings.

References

1. Van der Berg, J. D. J. *Analytical chemical studies on traditional linseed oil paints*, PhD Thesis, University of Amsterdam, (2002).
2. Croll, S. *Overview of development in the paint industry since 1930*, Modern paints Uncovered: proceeding from the Modern, Paints Uncovered Symposium, pp. 17–29, (2006).
3. Zerbe, K. *The Artist's Handbook Of Materials and Techniques*, Parnassus, vol.13, no.5, pp. 178–179 (1941).
4. Maroger, J. *The secret formules and techniques of the masters*, London/NewYork, (1948).
5. Izzo, F. C. *20th century artists' oil paint: a chemical-physical survey*, PhD thesis, University of Ca' FoscariUniversity, Venice, (2011).
6. Casadio, F. et al. *Metal Soaps in Art: Conservation and Research*, Springer International Publishing - Herit Sci, 2019.
7. Henderson, J. Managing uncertainty for preventive conservation. *Stud. Conserv* **63**, 108–112 (2018).
8. Lazzari, M. & Chiantore, O. Drying and oxidative degradation of linseed oil. *Polym. Degrad. Stab.* **65**, 303–313 (1999).
9. Fjallstrom, P., Andersson, B., Nilsson, C. & Andersson, K. Drying of linseed oil paints: a laboratory study of aldehyde emission. *Ind. Crops Products* **16**, 174–184 (2002).
10. Tumosa, C. S., Mecklenburg, M. F., Oil Paints: The Chemistry of Drying Oils and the Potential for Solvent Disruption, New Insights into the Cleaning of Paintings: Proceedings from the Cleaning 2010 International Conference, Universidad Politecnica de Valencia and Museum Conservation Institute, no. 2010, pp. 51–58, 2013.
11. Pizzimenti, S. et al. Oxidation and cross-linking in the curing of air-drying artists' oil paints. *ACS Appl Polym. Mater.* **3**, 1912–1922 (2021).
12. Sawicka, L. et al. *Conservation of Modern Oil Paintings*, 2019).
13. Steele, L. L. Effect of certain metallic soaps on the drying of raw linseed oil. *Ind. Eng.* **16**, 957–959 (1924).
14. Izzo, F. C., Kratter, M., Nevin, A. & Zendri, E. A critical review on the analysis of metal soaps in oil paintings. *Chem. Open* **10**, 904–921 (2021).
15. Hermans, J. J., Keune, K., Van Loon, A., Iedema, P. D. Toward a Complete Molecular Model for the Formation of Metal Soaps in Oil Paints, pp. 47–67, 2019.
16. Spring, M., Higgitt, C. & Saunders, M. Investigation of pigment-medium interaction processes in oil paint containing degraded smalt. *Natl Gallery Tech. Bull.* **26**, 56–70 (2005).
17. Mecklenburg, M. F., Tumosa, C. S., Vicenzi, E. P. *The Influence of Pigments and Ion Migration on the Durability of Drying Oil and Alkyd Paints*, New Insights into the Cleaning of Paintings: Proceedings from the Cleaning 2010 International Conference, Universidad Politecnica de Valencia and Museum Conservation Institute, pp. 59–67, 2013.
18. Izzo, F. C., Zanin, C., van Keulen, H. & da Roit, C. From pigments to paints: Studying original materials from the atelier of the artist Mariano Fortuny y Madrazo. *Int. J. Conserv. Sci.* **8**, 547–564 (2017).
19. Cotte, M. et al. Lead soaps in paintings: Friends or foes? *Stud. Conserv* **62**, 2–23 (2017).
20. Tumosa, C. S. & Mecklenburg, M. F. The influence of lead ions on the drying of oils. *Stud. Conserv* **50**, 39–47 (2005).
21. Meneghetti, S. M. P., de Souza, R. F., Monteiro, A. L., de Souza, M. O. Substitution of lead catalysts by zirconium in the oxidative polymerization of linseed oil, Progress in Organic Coatings, pp. 219–224, 1998.
22. Osmond, G. *Zinc Soaps: An Overview of Zinc Oxide Reactivity and Consequences of Soap Formation in Oil-Based Paintings*. 2019.
23. Beerse, M., Keune, K., Iedema, P., Woutersen, S. & Hermans, J. Evolution of zinc carboxylate species in oil paint ionomers. *ACS Appl Polym. Mater.* **2**, 5674–5685 (2020).
24. Izzo, F. C. et al. Some considerations about selective damaged induced by pigment-medium interactions in a Neoplasticist oil canvas painting: Composition dans le cône avec couleur orange by G. (1929). *Herit. Sci.* **12**, 92 (2024).
25. Mecklenburg, M. F., Fuster, L., Failure Mechanisms in Canvas Supported Paintings: Approaches for Developing Consolidation Protocols, Colour and conservation: materials and methods in the conservation of polychrome artworks: third international conference, pp. 49–59, 2006.
26. Erhardt, D., Tumosa, C. S. & Mecklenburg, M. F. Long-term chemical and physical processes in oil paint films. *Stud. Conserv* **50**, 143–150 (2005).
27. Kékicheff, P. et al. Relationships between chemical and physical alterations of historical oil-based pictorial paintings: craquelures and metal ion-migration, From Soft Matter to Biophysics 2023, Book of abstract, pp. 29, 2023.
28. Vila, A. et al., Picasso 1917: An Insight into the Effects of Ground and Canvas in the Failure Mechanisms in Four Artworks, Conservation of Modern Oil Paintings, pp. 245–253, 2019.
29. Chen-Wiegart, Y. K. et al. Elemental and molecular segregation in oil paintings due to lead soap degradation. *Sci. Rep.* **7**, 1–9 (2017).
30. Eumelen, G. J. A. M. et al. Computational modelling of metal soap formation in historical oil paintings: the influence of fatty acid concentration and nucleus geometry on the induced chemo-mechanical damage, *SN Appl Sci*, 2, no. 7, 2020.
31. van Driel, B. A. et al. Determination of early warning signs for photocatalytic degradation of titanium white oil paints by means of surface analysis. *Spectrochim. Acta A Mol. Biomol. Spectrosc.* **172**, 100–108 (2017).
32. Mecklenburg, M. F., Tumosa, C. S., Vicenzi, E. P., *The Influence of Pigments and Ion Migration on the Durability of Drying Oil and Alkyd Paints*, New Insights into the Cleaning of Paintings: Proceedings from the Cleaning 2010 International Conference, Universidad Politecnica de Valencia and Museum Conservation Institute, pp. 59–67, 2013.
33. Fuster-López, L. et al., Selective cracks: Mapping damage from pigment-medium interaction in three neo-plastic oil paintings, *Working Towards a Sustainable Past. ICOM-CC 20th Triennial Conference Preprints, Valencia*, 2023.
34. Watson, G., *The Process of Alkali Refining Linseed Oil*, Published by Golden Artist Colors, Inc, 2018.
35. Consultation on 23-04-2022, "Golden Paint Inc."
36. *Standard Test Methods for Evaluating Drying or Curing During Film Formation of Organic Coatings Using Mechanical Recorders (ASTM D5895-20)*, Book of Standard.
37. dePolo, G., Walton, M., Keune, K. & Shull, K. R. After the paint has dried: a review of testing techniques for studying the mechanical properties of artists' paint. *Herit. Sci.* **9**, 1–24 (2021).
38. Ciccola, A., Guiso, M., Domenici, F., Sciubba, F. & Bianco, A. Azo-pigments effect on UV degradation of contemporary art pictorial film: A FTIR-NMR combination study. *Polym. Degrad. Stab.* **140**, 74–83 (2017).
39. Fuster-López, L., Izzo, F. C., Damato, V., Yusà-Marco, D. J. & Zendri, E. An insight into the mechanical properties of selected commercial oil and alkyd paint films containing cobalt blue. *J. Cultural Herit.* **35**, 225–234 (2019).

40. Fuster-López, L. et al. Study of the chemical composition and the mechanical behaviour of 20th century commercial artists' oil paints containing manganese-based pigments. *Microchem. J.* **124**, 962–973 (2016).

41. Izzo, F. C. et al. 20th century artists' oil paints: The case of the Olii by Lucio Fontana. *J. Cultural Herit.* **15**, 557–563 (2014).

42. Izzo, F. C., Van Den Berg, K. J., Van Keulen, H., Ferriani, B., Zendri, E., Moder Oil Paints-Formulations, Organic Additives and Degradation: Some Case Studies, Issues in Contemporary Oil Paint, Book of abstract, pp. 75–104, 2014.

43. López-Ramírez, M. R., Navas, N., Rodríguez-Simón, L. R., Otero, J. C. & Manzano, E. Study of modern artistic materials using combined spectroscopic and chromatographic techniques. Case study: Painting with the signature 'Picasso. *Anal. Methods* **7**, 1499–1508 (2015).

44. Juita, B., Dlugogorski, E. Z., Kennedy, E. & Mackie, J. Oxidation reactions and spontaneous ignition of linseed oil. *Proc. Combust. Inst.* **33**, 2625–2631 (2011).

45. Tumosa, C. S. & Meckelnburg, M. Weight changes on oxidation of drying and semi-drying oils. *Collect. Forum* **18**, 116–123 (2003).

46. Izzo, F. C., Zendri, E., Biscontin, G. & Balliana, E. TG-DSC analysis applied to contemporary oil paints. *J. Therm. Anaysis Calorimetri* **104**, 541–546 (2011).

47. Palladino, N. et al. An analytical survey of zinc white historical and modern artists' materials. *Herit. Sci.* **12**, 1–29 (2024).

48. Omari, A., Mgani, Q. A., Mubofu, E. B. Fatty Acid Profile and Physico-Chemical Parameters of Castor Oils in Tanzania, Green and Sustainable Chemistry, 5, no.4, 2015.

49. Baij, L., Hermans, J. J., Keune, K. & Iedema, P. Time-dependent ATR-FTIR spectroscopic studies on fatty acid diffusion and the formation of metal soaps in oil paint model systems. *Angew. Chem. - Int. Ed.* **57**, 7351–7354 (2018).

50. Osmond, G. Zinc white: a review of zinc oxide pigment properties and implications for stability in oil-based paintings, *Metal Soap in Art*, pp. 25–46, 2019.

51. Artesani, A. Zinc oxide instability in drying oil paint, Materials Chemistry and Physics, vol. 255. Elsevier Ltd, Nov. 15, 2020.

52. van Driel, B. et al. New insights into the complex photoluminescence behaviour of titanium white pigments. *Dyes Pigments* **155**, 14–22 (2018).

53. Cucci, C., Picollo, M., Stefani, L. & Jiménez, R. The man who became a Blue Glass. Reflectance hyperspectral imaging discloses a Picasso painting of the Blue period. *J. Cult. Herit.* **62**, 484–492 (2023).

54. Bonaduce, I. et al. A multi-analytical approach to studying binding media in oil paintings: Characterisation of differently pre-treated linseed oil by DE-MS, TG and GC/MS. *J. Therm. Ananalysis Calorim.* **107**, 1055–1066 (2012).

55. Bonaduce, I. et al. New insights into the ageing of linseed oil paint binder: a qualitative and quantitative analytical study. *PLoS ONE* **7**, e49333 (2012).

56. Modugno, F. et al. On the influence of relative humidity on the oxidation and hydrolysis of fresh and aged oil paints. *Sci. Rep.* **9**, 1–16 (2019).

57. Nardelli, F. et al. The stability of paintings and the molecular structure of the oil paint polymeric network. *Sci. Rep.* **11**, 1–14 (2021).

58. Macchia, A. et al. Combined Use of Non-Invasive and Micro-Invasive Analytical Investigations to Understand the State of Conservation and the Causes of Degradation of I Tesori del Mare (1901) by Plinio Nomellini. *Methods Protoc.* **5**, 1–18 (2022).

59. Giorgi, L. et al. In-situ technical study of modern paintings - Part 2: Imaging and spectroscopic analysis of zinc white in paintings from 1889 to 1940 by Alessandro Milesi (1856–1945). *Spectrochimica Acta Part A: Mol. Biomolecular Spectrosc.* **219**, 504–508 (2019).

60. Mallegol, J., Lemaire, J. & Gardette, J. Drier influence on the curing of linseed oil. *Prog. Org. Coat.* **39**, 107–113 (2000).

61. Stenberg, C., Svensson, M. & Johansson, M. A study of the drying of linseed oil with different fatty acid patterns using RTIR-Spetroscopy and chemiluminescence (CL). *Ind. Crops Prod.* **21**, 263–272 (2005).

62. Matteini, M., Moles, A., *Scienza e restauro. Metodi d'indagine*, 7th ed., vol. Arte e restauro. 1994.

63. Vagnini, M., Gabriel, F., Daveri, A., Sali, D., Handheld new technology Raman and portable FT-IR spectrometers as complementary tools for the in situ identification of organic materials in modern art, Spectrochimica Acta Part A: Molecular and Biomolecular Spectroscopy, 176, Apr. 2017.

64. Berthomieu, C. & Hienerwadel, R. Fourier transform infrared (FTIR) spectroscopy. *Photosynthesis Res.* **101**, 157–170 (2009).

65. Giorgi, L. et al. In-situ technical study of modern paintings part 1: The evolution of artistic materials and painting techniques in ten paintings from 1889 to 1940 by Alessandro Milesi (1856–1945). *Spectrochimica Acta Part A: Mol. Biomolecular Spectrosc.* **219**, 530–538 (2019).

66. Andersen, C. K., et al. Mechanical and Moisture Sorption Properties of Commercial Artists' Oil Paint by Dynamic Mechanical Thermal Analysis (DMA), Nanoindentation, and Dynamic Vapour Sorption (DVS), Conservation of Modern Oil Paintings, pp. 403–418, 2019.

67. Lee, D. S. H. et al. Numerical modelling of mechanical degradation of canvas paintings under desiccation. *Herit. Sci.* **10**, 1–13 (2022).

68. Ploeger, R., Scalarone, D. & Chiantore, O. The characterization of commercial artists' alkyd paints. *J. Cultural Herit.* **9**, 412–419 (2008).

Acknowledgements

Author contributions

Conceptualization, L.F.L., M.M., and F.C.I; methodology, M.G., L.F.L., and F.C.I; software and analyses, M.G, L.F.L., and F.C.I; validation, M.G, L.F.L, M.M. and F.C.I; investigation, M.G., L.F.L., and F.C.I; resources, L.F.L, S.S., G.W., and F.C.I; data curation, M.G., L.F.L., and F.C.I; writing—original draft preparation, M.G., L.F.L., M.M., A.M., S.S., G.W., and F.C.I; writing—review and editing, M.G., L.F.L., M.M., A.M., S.S., G.W., and F.C.I.; project administration, L.F.L. and F.C.I.; funding acquisition, L.F.L. All authors have read and agreed to the published version of the manuscript.

Competing interests

The authors declare no competing interests.

Ethical Approval

Not applicable.

Additional information